J. Fluid Mech. (1987), *vol.* 176, *pp.* 283–293
Printed in Great Britain

Weir flows

By JEAN-MARC VANDEN-BROECK
Department of Mathematics and Mathematics Research Center, University of Wisconsin-Madison, Madison, WI 53706, USA

AND JOSEPH B. KELLER
Departments of Mathematics and Mechanical Engineering, Stanford University, Stanford, CA 94305, USA

(Received 23 January 1986 and in revised form 1 May 1986)

The flow of a liquid with a free surface over a weir in a channel is calculated numerically for thin weirs in channels of various depths, and for broad-crested weirs in channels of infinite depth. The results show that the upstream velocity, as well as the entire flow, are determined by the height of the free surface far upstream and by the geometry of the weir and channel, in agreement with observation. The discharge coefficient is computed for a thin weir, and a formula for it is given that applies when the height of the weir is large compared to the height of the upstream free surface above the top of the weir. The coefficients in this formula are close to those found empirically.

1. Introduction

The flux or discharge Q of fluid along a channel is the product of the fluid mean velocity U and cross-sectional area $A(H)$, which depends upon the free-surface level H:

$$Q = UA(H). \tag{1.1}$$

Both U and H must be known to determine Q from (1.1). However observation shows that in a channel partially obstructed by a weir, Q is determined by H alone. Then Q can be found without measuring U, which is one of the reasons for using weirs (Ackers *et al.* 1978).

This observation implies that although U and H are independent in an unobstructed channel, they are not independent in a channel containing a weir. Instead $U = U(H)$ is a function of H and of the size and shape of the weir. Up to the present, this rather surprising fact has not been treated hydrodynamically.

To analyse it, we shall calculate numerically the flows over thin two-dimensional weirs in channels of different depths, and over broad-crested two-dimensional weirs in channels of infinite depth. This requires solving free-surface problems in the presence of gravity. For this purpose we assume that the fluid is incompressible and inviscid, and that each flow is irrotational, steady and two-dimensional. We also assume that there are no surface waves.

For a thin weir at each surface height H we find that there is a solution for only one value of U, which depends upon H and upon the height W of the weir. This confirms the empirical result mentioned above. We determine the flux Q, the discharge coefficient C, and the shape of the free surface for this solution. We also obtain a formula for C when H/W is small, where H is measured from the top of the weir. This formula is of the form used in practice, and the computed coefficients in it are close to the empirical ones (Ackers *et al.* 1978).

For a broad-crested weir of length L and height $W = \infty$, we find that there is a unique flow for given values of H and L. We determine Q, C and the free surface for two values of H/L.

In §2 we define C and introduce the form of the equation for it. Then in §3 we consider a thin weir in a channel of infinite depth. After formulating the flow problem mathematically, we present our numerical procedure for solving it and display some of the numerical results. In §4 we treat a thin weir in a channel of finite depth while in §5 we treat broad-crested weirs in a channel of infinite depth. Finally in §6 we discuss a related free-surface flow that can be analysed explicitly, and discuss some of the relevant literature.

2. Discharge coefficient

Figure 1 (*a*) shows a side view of a channel with a thin weir, and figure 1 (*b*) shows a cross-section of the channel at the weir. The height H of the free surface far upstream and the depth W of the bottom are measured from some point on the upper edge of the weir, as is shown in figure 1 (*a*). The cross-sectional area $A(H)$ of the channel, and the area $a(H)$ of the region above the weir up to the level H, are shown in figure 1 (*b*).

In terms of these quantities and the acceleration due to gravity g, we define the dimensionless discharge coefficient C by

$$Q = C(gH)^{\frac{1}{2}} a(H). \tag{2.1}$$

The fact that the flow is determined by H means that C is a function only of H and of the geometry of the weir and the channel. Since C is dimensionless, we shall write it as a function of the dimensionless ratio $H/W, C = C(H/W)$. It also depends upon other dimensionless geometrical parameters.

We assume that C is regular for H/W small, so that it has the form

$$C\left(\frac{H}{W}\right) = C(0) + C'(0)\frac{H}{W} + O\left[\left(\frac{H}{W}\right)^2\right]. \tag{2.2}$$

For flows over two-dimensional thin weirs this assumption is confirmed by our numerical results, which are presented in §§3 and 4. The results also determine the coefficients $C(0)$ and $C'(0)$ for those particular weirs.

Let us specialize these formulas to a weir with a rectangular opening of width b, for which $a(H) = bH$. Then (2.1) and (2.2) yield

$$Q = g^{\frac{1}{2}} H^{\frac{3}{2}} b \left\{C(0) + C'(0)\frac{H}{W} + O\left[\left(\frac{H}{W}\right)^2\right]\right\}. \tag{2.3}$$

For a weir with a V-notch of angle $\theta, a(H) = H^2 \tan\frac{1}{2}\theta$ and we get instead

$$Q = g^{\frac{1}{2}} H^{\frac{5}{2}} \tan\tfrac{1}{2}\theta \left\{C_V(0) + C'_V(0)\frac{H}{W} + O\left[\left(\frac{H}{W}\right)^2\right]\right\}. \tag{2.4}$$

Results of the forms (2.3) and (2.4) are used in practice (Ackers *et al.* 1978). They are derived by dimensional analysis, hydraulic approximations and fitting to experimental data. Corrections for viscous and surface-tension effects are often included.

By combining (1.1) and (2.1), we can determine the velocity U. From it we find

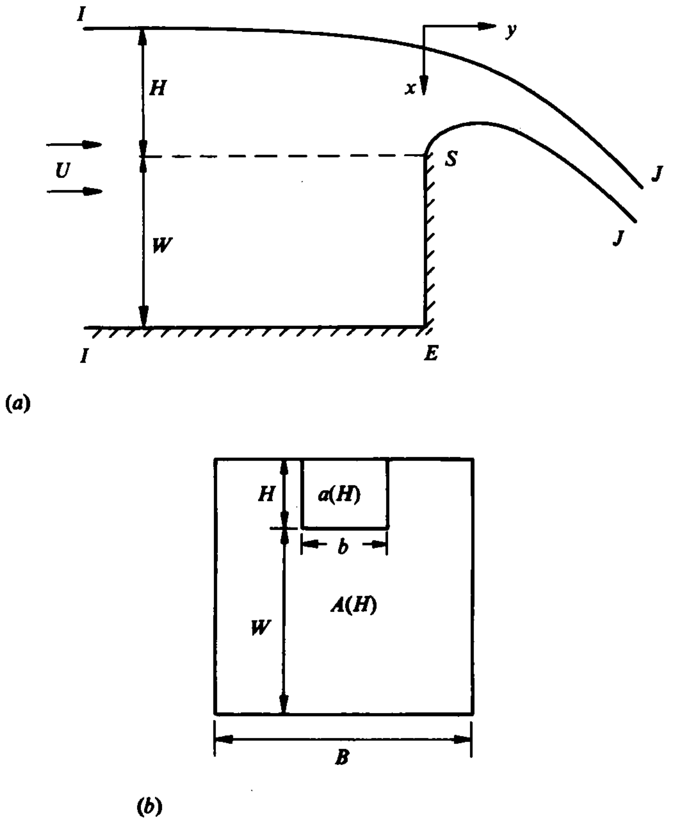

FIGURE 1. (*a*) Side view of a channel with a thin weir. (*b*) Cross-section of a rectangular channel of width B at the weir, which has a rectangular opening of width b, at height W above the bottom. The water depth far upstream is $W+H$.

that the Froude number $F = U[g(H+W)]^{-\frac{1}{2}}$ of the flow in the channel, based upon the total depth, is

$$F = C\left(\frac{H}{W}\right)\left(1+\frac{W}{H}\right)^{-\frac{1}{2}}\frac{a(H)}{A(H)}$$
$$= \frac{a(H)}{A(H)}\left(\frac{H}{W}\right)^{\frac{1}{2}}\left\{C(0)+[C'(0)-\tfrac{1}{2}C(0)]\frac{H}{W}+O\left[\left(\frac{H}{W}\right)^{2}\right]\right\}. \tag{2.5}$$

For a weir with a rectangular opening of width b in a rectangular channel of width B, we have $a(H) = bH, A(H) = B(H+W)$ and (2.5) becomes

$$F = \frac{b}{B}\left(\frac{H}{W}\right)^{\frac{3}{2}}\left\{C(0)+[C'(0)-\tfrac{3}{2}C(0)]\frac{H}{W}+O\left[\left(\frac{H}{W}\right)^{2}\right]\right\}. \tag{2.6}$$

For a thin weir, the only other geometrical ratios upon which $C(0)$ and $C'(0)$ depend in this case are b/B and the lateral position of the opening. This result shows that F is small, of order $(H/W)^{\frac{3}{2}}$, when H/W is small, so then the flow is extremely subcritical. When $b = B$ the flow is two-dimensional and then the coefficients are constants. We shall determine them in §§3 and 4.

3. Thin weir in infinitely deep channel

Let us consider a thin weir, such as that shown in figure 1 (*a*), in a channel of infinite depth, so that $W = \infty$. Let the channel be rectangular with width $B = b$, so that the opening above the weir extends completely across the channel. Then the flow is two-dimensional. We seek a flow that becomes a falling jet with two free surfaces after it crosses the weir. Thus the flow appears as in figure 1 (*a*) with the bottom removed to infinity, and with the jet falling to infinity.

We introduce Cartesian coordinates with the x-axis directed vertically downwards through the separation point S, and with the asymptote to the upper free surface as the y-axis (see figure 1*a*). Gravity acts in the x-direction. As $y \to -\infty$, the velocity approaches zero. As $y \to +\infty$ the flow approaches the thin-jet solutions of Keller & Weitz (1957) and Keller & Geer (1973).

Let the potential function be ϕ and the stream function be ψ. Without loss of generality we choose $\psi = 0$ on the lower free surface and $\phi = 0$ at the separation point S. Let Q be the value of ψ on the upper free surface. On the two free surfaces the Bernoulli equation yields

$$\tfrac{1}{2}(\nabla\phi)^2 - gx = 0. \tag{3.1}$$

We introduce dimensionless variables by taking $(Q^2/g)^{\frac{1}{3}}$ as the unit length and $(Qg)^{\frac{1}{3}}$ as the unit velocity. In these new variables (3.1) becomes

$$(\nabla\phi)^2 - 2x = 0 \quad \text{on} \begin{cases} \psi = 1 \\ \psi = 0, \phi > 0. \end{cases} \tag{3.2}$$

The plane of the dimensionless potential $f = \phi + \mathrm{i}\psi$ is shown in figure 2.

Let the complex velocity be $\zeta = u - \mathrm{i}v$. Here u and v are the x- and y-components of the vector velocity. As $f \to -\infty$, we require that there be no waves, so the velocity ζ vanishes like e^f. As $f \to +\infty$, the velocity ζ increases like $f^{\frac{1}{3}}$ (Keller & Weitz 1957). Thus we have

$$\zeta \sim \mathrm{e}^f \quad \text{as}\, f \to -\infty, \tag{3.3}$$

$$\zeta \sim f^{\frac{1}{3}} \quad \text{as}\, f \to +\infty. \tag{3.4}$$

The problem is to find ζ as an analytic function of $f = \phi + \mathrm{i}\psi$ in the strip $0 < \psi < 1$, satisfying (3.2)–(3.4) and the kinematic condition

$$v = 0 \quad \text{on}\ \psi = 0, \phi < 0. \tag{3.5}$$

We define the new variable t by the relation

$$f = \frac{1}{\pi} \ln \frac{(t+1)^2}{2(t^2+1)}. \tag{3.6}$$

The transformation (3.6) maps the flow domain into the interior of the unit circle in the t-plane so that the vertical wall goes onto the real diameter and the free surface goes onto that portion of the circumference lying in the upper half of the t-plane (see figure 3).

Following de Boor (1961) we define the function $\Omega(t)$ by the relation

$$\zeta = -(t+1)\left[-\ln c(1+t^2)\right]^{\frac{1}{3}} \mathrm{e}^{\Omega(t)}. \tag{3.7}$$

Here c is a real constant between 0 and $\frac{1}{2}$. We shall choose $c = 0.2$. It can be checked easily that the expression (3.7) satisfies the conditions (3.3) and (3.4). The function $\Omega(t)$ is analytic for $|t| < 1$ and continuous for $|t| \leqslant 1$. The kinematic condition (3.5) implies that the expansion of $\Omega(t)$ in powers of t has real coefficients. With this

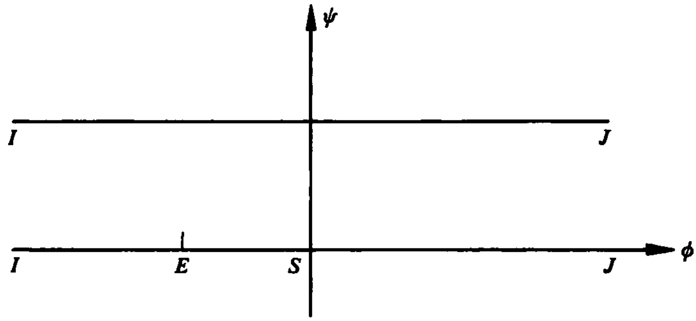

FIGURE 2. The complex potential plane. For a thin weir in an infinitely deep channel, the point E coincides with I at $-\infty$. For a channel of finite depth, E is on the axis between I and S, as it is also for a broad-crested weir in a channel of infinite depth.

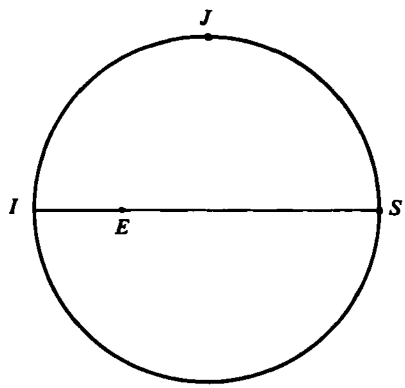

FIGURE 3. The complex t-plane. For a thin weir in an infinitely deep channel, E coincides with I at $t = -1$. For a channel of finite depth E is on the diameter between I and S. The same is true for a broad-crested weir in a channel of infinite depth.

expansion inserted, (3.7) becomes

$$\zeta = -(t+1)\,[-\ln c(1+t^2)]^{\frac{1}{3}} \exp\left(\sum_{n=0}^{\infty} U_n t^n\right). \tag{3.8}$$

The function (3.8) satisfies (3.3)–(3.5). The unknown real coefficients U_n have to be determined to make (3.8) satisfy the Bernoulli condition (3.2).

We use the notation $t = |t|\,e^{i\sigma}$ so that points on the free surfaces are given by $t = e^{i\sigma}$, $0 < \sigma < \pi$. Using (3.6) and the identity

$$\frac{\partial x}{\partial \phi} + i\frac{\partial y}{\partial \phi} = \frac{1}{\zeta} \tag{3.9}$$

we obtain after some algebra

$$\frac{d\tilde{x}}{d\sigma} = \frac{1}{2\pi}\frac{\sin\sigma}{\cos\sigma\,\cos^2\frac{1}{2}\sigma}\,\frac{\tilde{u}(\sigma)}{\tilde{u}(\sigma)^2+\tilde{v}(\sigma)^2}, \tag{3.10}$$

$$\frac{d\tilde{y}}{d\sigma} = \frac{1}{2\pi}\frac{\sin\sigma}{\cos\sigma\,\cos^2\frac{1}{2}\sigma}\,\frac{\tilde{v}(\sigma)}{\tilde{u}(\sigma)^2+\tilde{v}(\sigma)^2}. \tag{3.11}$$

Here $\tilde{\zeta}(\sigma) = \tilde{u}(\sigma) - i\tilde{v}(\sigma)$ denotes the value of ζ at a point on a free surface.

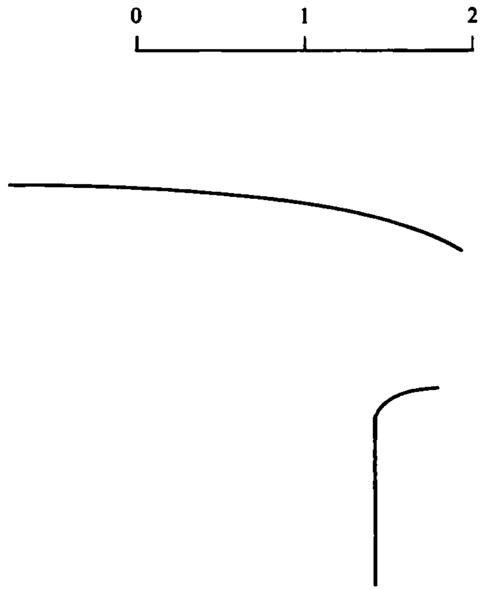

FIGURE 4. Computed free-surface profile for the flow past a thin weir in an infinitely deep channel. The vertical scale is the same as the horizontal scale.

The value of $\tilde{x}(\sigma)$ on the free surface is obtained by integrating (3.10):

$$\tilde{x}(\sigma) = x_S + \int_0^{\sigma} \frac{1}{2\pi} \frac{\sin\tau}{\cos\tau\cos^2\frac{1}{2}\tau} \frac{\tilde{v}(\tau)}{\tilde{u}(\tau)^2+\tilde{v}(\tau)^2} \mathrm{d}\tau, \quad 0 < \sigma < \tfrac{1}{2}\pi, \tag{3.12}$$

$$\tilde{x}(\sigma) = \int_{\pi}^{\sigma} \frac{1}{2\pi} \frac{\sin\tau}{\cos\tau\cos^2\frac{1}{2}\tau} \frac{\tilde{v}(\tau)}{\tilde{u}(\tau)^2+\tilde{v}(\tau)^2} \mathrm{d}\tau, \quad \tfrac{1}{2}\pi < \sigma < \pi. \tag{3.13}$$

Here x_S is the value of x at the separation point S.

We solve for the U_n numerically by truncating the infinite series in (3.8) after N terms. For convenience we choose N to be even. To get equations for the coefficients U_n we use collocation. Thus we introduce the N mesh points

$$\sigma_I = \frac{\pi}{2N} + \frac{\pi}{N}(I-1) \quad (I = 1, \ldots, N).$$

Using (3.8), (3.12) and (3.13) we obtain $\zeta(\sigma_I)$ and $\tilde{x}(\sigma_I)$ in terms of the coefficients U_n and x_S. Substituting these expressions into (3.2) at the point σ_I, we obtain N nonlinear algebraic equations for the $N+1$ unknowns $x_S, U_1, U_2, \ldots, U_N$. Another equation is obtained by integrating $\partial x/\partial\psi$ along the equipotential $\phi = 0$ from $\psi = 0$ to 1 and equating the value of x at $\psi = 1$ to the corresponding value of $\tilde{x}(\sigma)$ obtained from (3.12).

We solve this system by Newton's method. Once it is solved, we obtain the shape of the free surfaces in parametric form by integrating numerically (3.10) and (3.11). A typical profile obtained in this way is shown in figure 4.

To determine the coefficient $C(0)$, which occurs in (2.3), we calculate x_S, the x coordinate of the separation point S. It follows from (2.3) and our choice of dimensionless variables that $C(0)$ is related to x_S by

$$C(0) = x_S^{-\frac{3}{2}}. \tag{3.14}$$

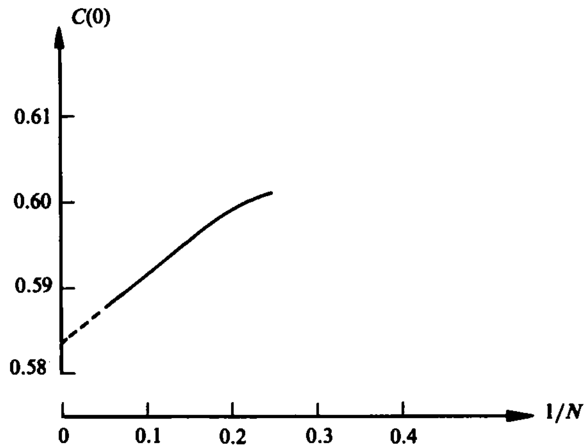

FIGURE 5. Numerical values of $C(0)$ versus $1/N$ obtained by the scheme of §3. The broken line corresponds to a linear extrapolation to $N = \infty$.

By using (3.14) and the calculated values of x_S, we have computed $C(0)$ for different numbers of mesh points N. Figure 5 is a graph of the values of $C(0)$ versus $1/N$. It indicates that $C(0)$ varies linearly with $1/N$ for N large. The broken line in figure 5 represents a linear extrapolation to $N = \infty$, which gives

$$C(0) \sim 0.583. \tag{3.15}$$

The value of $C'(0)$ will be obtained in the next section.

4. Thin weir in channel of finite depth

We now generalize the procedure of §3 to include the effect of finite depth, so that $W \neq \infty$ (see figure 1*a*). The dimensionless potential plane is shown in figure 2. By using the transformation (3.6), we map the flow domain into the interior of the unit circle in the t-plane, so that the horizontal bottom and the vertical wall go respectively onto the portions IE and ES of the real diameter. The free surface goes onto the portion of the circumference lying in the upper half of the t-plane (see figure 3).

We denote by $-e_0$ the value of t corresponding to the corner E. As $t \to -e_0$, the complex velocity vanishes like $(t+e_0)^{\frac{1}{2}}$. Therefore we can solve the problem numerically by using the procedure outlined in §3 with the relation (3.7) replaced by

$$\zeta = -(t+e_0)^{\frac{1}{2}}[-\ln c(1+t^2)]^{\frac{1}{3}}\, e^{\Omega(t)}. \tag{4.1}$$

As in §3 we chose $c = 0.2$.

We note that $\zeta \to$ constant as $t \to -1$. Therefore our formulation requires that there be no waves on the free surface. It follows from the choice of the dimensionless variables that the Froude number F is related to the value $\zeta(-1)$ of ζ at $t = -1$ by the relation

$$F = [\zeta(-1)]^{\frac{3}{2}}. \tag{4.2}$$

The procedure of §3 yields $N+1$ equations for the $N+2$ unknown $x_S, e_0, U_1, \ldots, U_N$. Another equation is obtained by using (4.2) where the Froude number F is specified. A typical profile, for $F = 0.1$, is shown in figure 6. The corresponding value of H/W is found to be 0.42. As $F \to 0$ we find that $e_0 \to -1$ and the solutions approach the solution presented in §3.

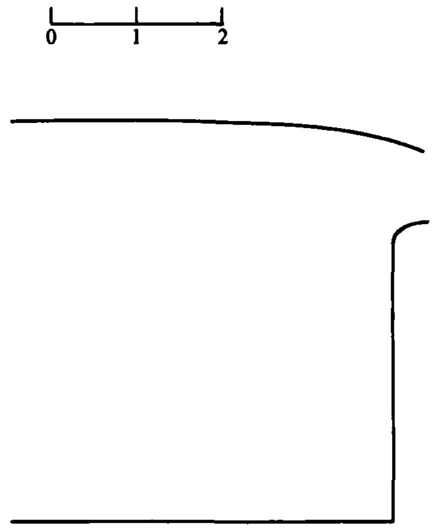

FIGURE 6. Computed free-surface profile for the flow past a thin weir in a channel of finite depth for $F = 0.1$. The vertical scale is the same as the horizontal scale.

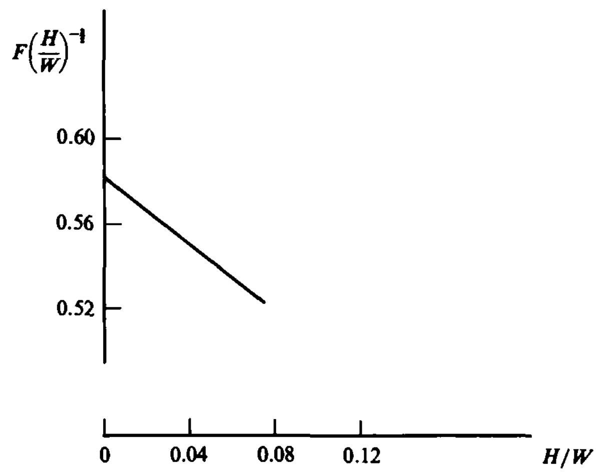

FIGURE 7. Values of $F(H/W)^{-\frac{3}{2}}$ versus H/W.

In order to check the formula (2.6) and to determine the coefficients $C(0)$ and $C'(0)$, we plot $F(H/W)^{-\frac{3}{2}}$ versus H/W in figure 7 for small values of H/W. These values were obtained by using the extrapolation procedure of figure 5. The curve in figure 7 is very close to a straight line of slope -0.80 which intersects the vertical axis at 0.583. Therefore

$$C(0) \sim 0.583, \tag{4.3}$$

$$C'(0) - \tfrac{3}{2}C(0) \sim -0.80. \tag{4.4}$$

The value of $C(0)$ predicted by (4.3) agrees with the value obtained in §3, (3.15). From (4.3) and (4.4) we find

$$C'(0) \sim 0.07. \tag{4.5}$$

Ackers *et al.* (1978, p. 57) present experimental values of C obtained by various investigators for $H/W = 0$ and for $H/W = 1$. As (2.2) shows, these are just the values of $C(0)$ and $C(0)+C'(0)+\ldots$. From the values listed in their table 3.1 we find that the experimental values of $C(0)$ and $C'(0)$ are in the ranges

$$0.564 \leqslant C(0) \leqslant 0.591, \tag{4.6}$$

$$0.066 \leqslant C'(0) \leqslant 0.085. \tag{4.7}$$

Our numerical results (4.3) and (4.5) are evidently within these experimental ranges.

5. Broad-crested weir in water of infinite depth

We shall now extend the procedures of §§3 and 4 to obtain the flow past a broad-crested weir in water of infinite depth (see figure 8). We denote by L the dimensionless length of the weir and we write the flux Q in the form (2.1) with the discharge coefficient $C_B(H/L)$. The dimensionless potential plane and the complex t-plane are the same as in §4 (see figures 2 and 3).

As $t \to -e_0$, the complex velocity ζ grows like $(t+e_0)^{-\frac{1}{3}}$. As $t \to -1$, ζ vanishes like $t+1$. Therefore we replace (4.1) by

$$\zeta = \mathrm{i}[-\ln c(1+t^2)]^{\frac{1}{3}}\,(t+1)\,(t+e_0)^{-\frac{1}{3}}\,\mathrm{e}^{\Omega(t)}. \tag{5.1}$$

We then follow step by step the procedure of §4 with (4.2) replaced by an equation that expresses the fact that the distance between E and S is equal to L. This equation is found by integrating numerically the identity (3.9) along the streamline $\psi = 0$ between E and S. Then C_B is found from (3.14).

A typical profile for $H/L = 0.88$ is shown in figure 8. A similar profile was found for $H/L = 1.23$. The corresponding values of the discharge coefficient are

$$C_B(0.88) = 0.583, \tag{5.2}$$

$$C_B(1.23) = 0.617. \tag{5.3}$$

These results indicate that for broad-crested weirs, the discharge Q depends only on H and on the geometry of the weir and of the channel.

6. Discussion

The weir flows that we have found in §§3–5 are subcritical free-surface flows without waves. The condition that there be no waves, which we imposed in our formulation, was essential in determining a particular solution. Therefore it is of interest to consider a case that can be treated exactly, and that leads to results of the form (2.2) and (2.6).

We consider the flow in figure 9, which is bounded by one free streamline and two horizontal rigid walls. We assume that there are no waves and we integrate the x-component of the Euler equation of motion over the flow domain. Upon using the divergence theorem we obtain

$$\oint [u_{\mathrm{n}}\, u_x + (\rho^{-1}p + gy)\, n_x]\, \mathrm{d}s = 0. \tag{6.1}$$

This line integral around the boundary of the flow domain can be evaluated as follows. First the normal velocity u_{n} vanishes on the walls and on the free streamline, while $u_{\mathrm{n}} = u_x = U_1$ or U_2 on the vertical lines at $x = \pm\infty$. Next we see that the x-component of the unit normal vanishes on the walls while $yn_x\,\mathrm{d}s = y\,\mathrm{d}y$ can be integrated along the free streamline where $p = 0$. Finally $\rho^{-1}p + gy = g(H_2 - H_1)$ at

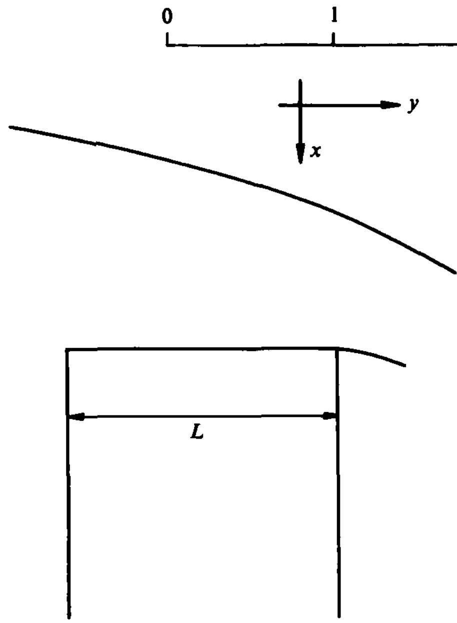

FIGURE 8. Computed free-surface profile for the flow past a broad-crested weir for $L = 1.6$. The vertical scale is the same as the horizontal scale.

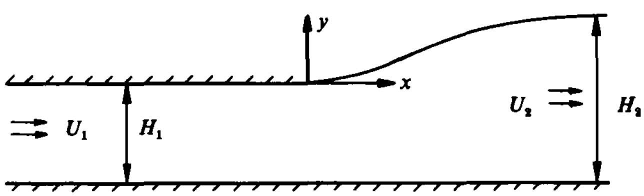

FIGURE 9. Sketch of a two-dimensional flow emerging from beneath a flat plate above a horizontal bottom.

$x = +\infty$ and $= g(H_2-H_1)+\frac{1}{2}(U_2^2-U_1^2)$ at $x = -\infty$ from the Bernoulli equation. Using all these facts in (6.1) we find

$$-U_1^2H_1-[\tfrac{1}{2}(U_2^2-U_1^2)+g(H_1-H_2)]H_1-\tfrac{1}{2}g(H_2-H_1)^2+U_2^2H_2+g(H_2-H_1)H_2 = 0. \tag{6.2}$$

Now we combine (6.2) with the mass conservation equation $U_1H_1 = U_2H_2$ to get

$$(H_2-H_1)^2(gH_1-U_2^2) = 0. \tag{6.3}$$

Thus either $H_2 = H_1$ or $U_2 = (gH_1)^{\frac{1}{2}}$. In the second case we see that the flow velocity is determined by the flow geometry. Then the Froude number $F = U_2(gH_2)^{-\frac{1}{2}}$ and the flux $Q = U_2H_2$ are also determined by the flow geometry. To exhibit the similarity of the results to those for a weir we set $H_1 = W$ and $H_2 = W+H$. Then we find

$$F = \left(1+\frac{H}{W}\right)^{-\frac{1}{2}} = 1-\frac{H}{2W}+O\left(\frac{H}{W}\right)^2, \tag{6.4}$$

$$Q = (gW)^{\frac{1}{2}}(W+H) = g^{\frac{1}{2}}W^{\frac{3}{2}}\left(1+\frac{H}{W}\right). \tag{6.5}$$

When $H > 0$ this flow is subcritical and without waves, just like the weir flows we have calculated. However for $H < 0$, the present flow is supercritical. For $F^2 = 2$ there is a stagnation point at $x = y = 0$ and the flow reduces to the configuration considered by Benjamin (1968). Vanden-Broeck (1980) has included waves in this problem for the particular case $W = \infty$, and calculated their amplitude by using this method.

In §4 we have found a unique subcritical flow for a thin weir of height W in a channel of finite depth $H+W$. In addition to this flow, there is a family of supercritical flows over the same weir in a channel of the same depth. For example when $F = \infty$, i.e. when gravity is negligible, there is an explicit free-boundary solution given by

$$\zeta = -(t+e_0)^{\frac{1}{2}}(te_0+1)^{-\frac{1}{2}}. \tag{6.6}$$

This solution can be used, together with the method of matched asymptotic expansions, to construct asymptotic expansions of solutions for $F \gg 1$. Presumably this family of solutions exists for all values of F greater than or equal to some critical value F_0.

Such asymptotic expansions were constructed for a waterfall, in which case $W = 0$ and $e_0 = -1$ in (6.6), by Clarke (1965) and by Keller & Geer (1973). More recently Goh & Tuck (1986) computed numerical solutions for waterfall flows emerging from between horizontal plates, and Tuck (1987) calculated the waterfall from a horizontal slot in a vertical wall. In all these cases the Froude number can be specified independently of the geometry. Finally we note that uniqueness theorems for weir flows are lacking. For flows under sluice gates some uniqueness results have been obtained by Budden & Norbury (1982).

The research of the first author was supported by the United States Army under contract DAAG 29-80-C-0041 and the National Science Foundation under Grant MCS-8001960. That of the second author was supported by the Office of Naval Research, the Air Force Office of Scientific Research, the Army Research Office and the National Science Founndation.

REFERENCES

Ackers, P., White, W. R., Perkins, J. A. & Harrison, A. J. M. 1978 *Weirs and Flumes for Flow Measurement*. Wiley.

Benjamin, T. B. 1968 *J. Fluid Mech.* **31**, 209.

Budden, P. & Norbury, J. 1982 *Arch. Rat. Mech. Anal.* **78**, 361.

Clarke, N. S. 1965 *J. Fluid Mech.* **22**, 359.

de Boor, C. 1961 *Project Report under Contract NONR-1866* (34), Harvard University, Cambridge, Mass.

Goh, K. H. M. & Tuck, E. O. 1985 *J. Engng Maths* **19**, 341.

Keller, J. B. & Geer, J. 1973 *J. Fluid Mech.* **59**, 417.

Keller, J. B. & Weitz, M. L. 1957 *Proc. Ninth Intl Cong. Appl. Mech.* **1**, 316.

Tuck, E. O. 1987 Efflux from a slit in a vertical wall. *J. Fluid Mech.* (in the press).

Vanden-Broeck, J.-M. 1980 *J. Fluid Mech.* **96**, 603.